Buckling Analysis of Ring-Stringer Stiffened Composite Cylinder

Nawras Haidar Mostafa

Abstract

Buckling of the stiffened composite cylinder is a very complex phenomenon that involves complex interactions between the skin and the stiffeners. Depending on different parameters, different buckling failure modes and failure loads are observed in stiffened composite cylinders. A 3-D finite elements model was built using ANSYS, which takes into consideration the exact geometric configuration and the orthotropic properties of the stiffeners and the shell. The effects of several parameters such as fiber orientation, shell thickness, and elastic material properties were carried out and general conclusions were drawn regarding the optimum configurations of the different parameters of the ring-stringer stiffened composite cylinder. The study corroborated that global buckling failure mode should be the design criteria for the stiffened composite cylinder.

الخلاصة:

يعتبر انبعاج الأسطوانة المقواة المصنوعة من المواد المركبة ظاهرة معقدة ناتجة عن التداخل المعقد بين القشرة و المقويات. بالاعتماد على بعض المتغيرات لوحظت أنماط و أحمال مختلفة للفشل.تم بناء النموذج ثلاثي الأبعاد باستخدام طريقة العناصر المحددة و المتمثلة بالبرنامج التحليلي (ANSYS) ، الذي أخذ بنظر الاعتبار الشكل الهندسي الحقيقي وخواص المادة المركبة للقشرة و المقويات وأجريت دراسة على بعض المتغيرات مثل زاوية تدوير الألياف و سمك القشرة ، و مواصفات المادة المركبة على الاسطوانة المقواة و التي أدت إلى ظهور نتائج تتعلق بأفضل ترتيب لأسطوانة مصنوعة من مواد مركبة تحتوي على مقويات طولية و حلقية و أكدت الدراسة على وجوب التصميم ضمن نطاق نمط الفشل بالانبعاج العام.

Nomenclatures

1-2-3	Material coordinate systems	
x-y-z	Nodal coordinate systems	
X-Y-Z	Global coordinate systems	
C_{ij}	Element of elasticity matrix to material axis	N/m^2
f	Shear correction factor	--
T^m	Transformation matrix	
Q_{ij}	Element of elasticity matrix.	N/m^2
u	Displacement	m
u_i	Nodal displacement in x-direction	m
$[K]^e$	Element stiffness matrix	N/m, N.m/rad
$\{a\}^e$	Element displacement vector	m
$[K]$	Overall stiffness matrix	N/m, N.m/rad
s-t-r	Local coordinate system	
$\{\varepsilon\}$	Strain vector	--
$\{\sigma\}$	Stress vector	N/m^2
υ_{ij}	Poisson's ratio through ij plane	--
$[E]$	Elasticity matrix	N/m^2
E_i	Elasticity modulus along i^{th} direction	N/m^2

1. Introduction

A composite material can be defined as a material that is composed of two or more distinct phases, usually a reinforcing material (filament) supported in compatible matrix, assembled in prescribed amounts to achieve specific physical and chemical properties (Stegman, J. and Lund, L, 2001). A basic ply or lamina of a fiber-reinforced composite material can be considered from macro-mechanical point of view as orthotropic material with two principal material directions or natural axis parallel and perpendicular to the direction of the filaments. By bonding these laminas together, a multi-laminas composite called laminate is formed.

Composite materials are desirable in lightweight structures due to their high specific stiffness and strength. Laminated composite materials provide the designer

with freedom to adapt the properties of the structure for given loads to obtain the maximum weight efficiency. However, high modulus and strength characteristics of composites result in structures with very thin sections that are often prone to buckling. Stiffeners are required to increase the bending stiffness of such thin walled members (plates, shells). Consequently, stiffened panels are often used in aircraft and launch vehicles to obtain lightweight structures with high bending stiffness. Stiffened shells are also more tolerant to imperfections and resist catastrophic growth of cracks. Cylindrical structures made of composite material are widely used in the above mentioned industries. Aircraft fuselage and launch vehicle fuel tanks are some of the many applications of these structures in aerospace and aircraft industries (Hatem H. O., 2002) such as in Figure (1). The advent of new manufacturing techniques in filament winding and automated fiber placement techniques as well as new innovative tooling concepts have decreased the manufacturing difficulties and hence have boosted the application of these composite cylinders (Langly, P. T. ,1989).

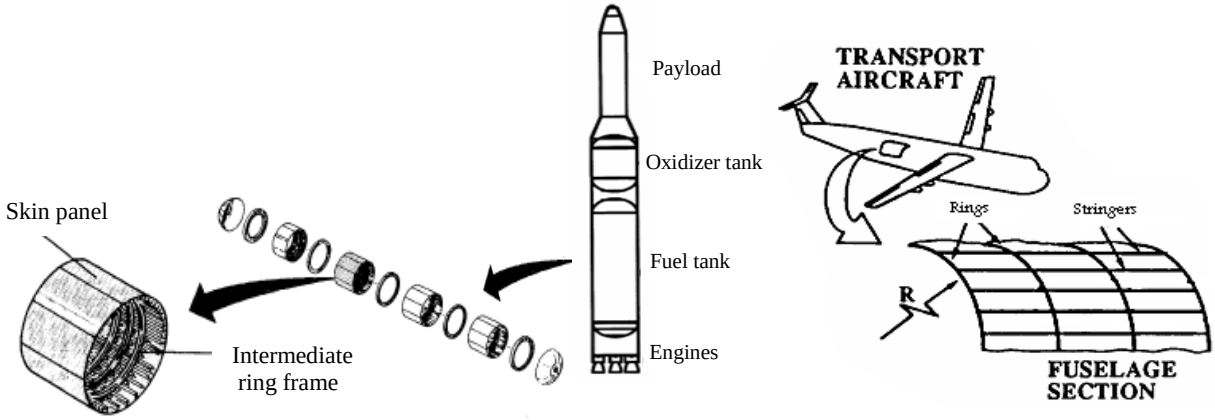

Figure (1): Stiffened panel configuration (Venkataraman, S., 1999 and Horak,J., *et al*, 2005).

Cylindrical shells are subjected to any combination of in plane, out of plane and shear loads during application. Minimizing the mass of shell structures has become a more important design consideration as the size of flight structures has increased. Large structures are often lightly loaded, and failure is frequently the result of buckling rather than of yielding (John, L *et al* 1972). Buckling failure mode of a stiffened cylindrical shell can further be subdivided into global buckling, local skin buckling and stiffener crippling. Global buckling is collapse of the whole structure, i.e. collapse of the stiffeners and the shell as one unit. Local skin buckling and stiffeners crippling on the other hand are localized failure modes involving local failure of only the skin in the first case and the stiffener in the second case. A stiffened cylinder will fail in any of these failure modes depending on the stiffener configuration, skin thickness, shell winding angle and type of applied load. Over the past four decades, a lot of research has been focused on the buckling, collapse, and post buckling behavior of cylindrical shells (Knight, N., and Stranes, J. 1997). A good portion of this work was devoted to the study of stiffened cylinders. The simplest stiffened cylinder consists of only axial stiffeners or stringers. A ring structure can be added to the stringers to achieve a better stiffened orthogrid configuration. A work by Graham ,J. (1993) presents analysis method for determining the buckling loads of ring and stringer stiffened cylinders. Another type of stiffener arrangement is the cross stiffeners arrangement (diamond shaped pattern). Phillips J.L. and Gurdal Z. (1990), discussed a smearing method for determining the global buckling load of this type of stiffened panels. Mostafa, N. H. and Waheed, S. O. (2008) studied the buckling

phenomenon of a composite cylinder with stringer stiffeners. The effects of shell winding angle, skin thickness, and material properties were investigated. Since the composite stiffened cylinder has important several applications especially in the aeronautical industries, thus it is an important to explore the optimum design (light weight with high strength) of such structures. The main object of this research is to extend the study that achieved by Mostafa, N. H. and Waheed, S. O. (2008) to investigate the effects of several parameters on the buckling load of a more complex stiffener construction including ring-stringer stiffened composite cylinder.

2 Finite Element Discritization

At present, the finite element method is the most powerful numerical technique, which offers an approximate solution to realistic types of structures. In the present study, the 8–nodded isoparametric quadrilateral and 20-noded structural solid elements are used for discritization of layered shell and layered stiffener respectively.

2.1 Element Parameters

A quadratic element named SHELL99 of quadrilateral shape as shown in Figure (2) consists of eight nodes, all of which are located on the element boundary have been used to define the shell finite element model, while that of rectangle shape consists of six nodes. These types of elements are used for plates and shells structure applications for membrane and flexural load conditions (Yunus, et al 1989). SOLID191 element shown in Figure (2) is a layered version of the 20-node structural solid designed to model layered thick shells or solids. The element is defined by 20 nodes having three degrees of freedom per node: translations in the nodal x, y, and z directions. SOLID191 has stress stiffening capabilities. This type of element is used to model the stiffeners that connected in the panel.

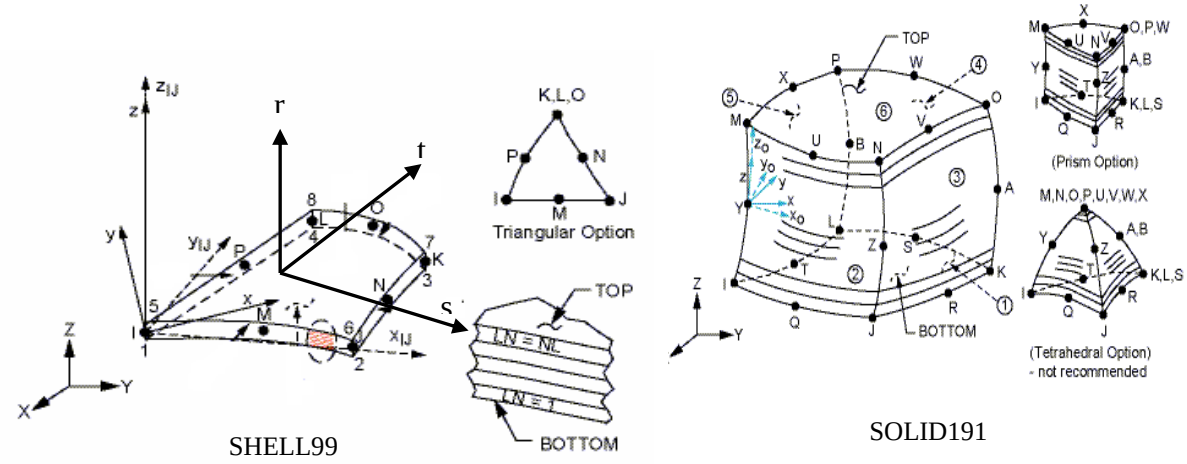

LN = Layer Number

NL = Total Number of Layers

Figure(2):Types of Elements geometry (ANSYS Element Reference,2004).

The displacement at any point within the element is written in terms of nodal translations and rotations as:

$$\begin{Bmatrix} u \\ v \\ w \end{Bmatrix} = \sum_{i=1}^{n} N_i \begin{Bmatrix} u_i \\ v_i \\ w_i \end{Bmatrix} + \sum_{i=1}^{n} N_i \frac{rt_i}{2} \begin{bmatrix} a_i^u & b_i^u \\ a_i^v & b_i^v \\ a_i^w & b_i^w \end{bmatrix} \begin{Bmatrix} \theta_{x,i} \\ \\ \theta_{y,i} \end{Bmatrix} \quad \text{… (1)}$$

Where, n is the number of element nodes.

N_i= shape functions.

u_i, v_i, w_i =global nodal displacements of node i.

{a}= unit vector in s direction.

{b}= unit vector in plane of element and normal to {a}.

$\theta_{x,i}$ = rotation of node i about vector {a}.

$\theta_{y,i}$ = rotation of node i about vector {b}.

t_i = nodal thickness.

r = natural coordinate along thickness direction but normal to the shell surface.

2.2 Mesh Generation

Figure (3) shows the proposed finite element model (stiffened cylinder), created using isoparametric shell elements of quadrilateral shapes. **ANSYS*** finite element program is used as a mathematical tool in the analysis of this model.

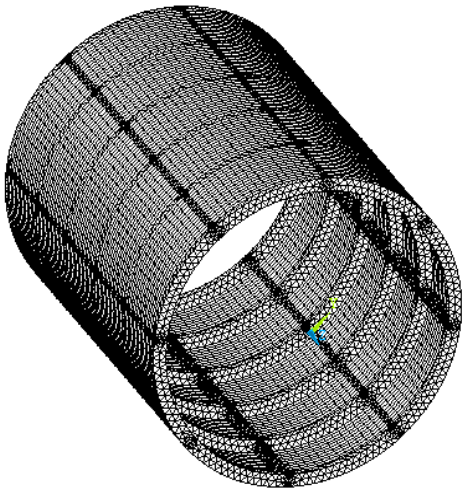

Figure (3): Meshed geometry

2.3 Stress Strain Relationship

Because of the linearly elastic behavior (assumption), the generalized Hooke's law is used for relating the stresses to strains. A material coordinate system is **x-y-z,** as shown in Figure (4) which introduced for the unidirectional reinforced lamina. Hook's law gives the general anisotropic constitutive relation with respect to a material coordinate system **1–2–3** as follows (Barbero E.J, 1999)

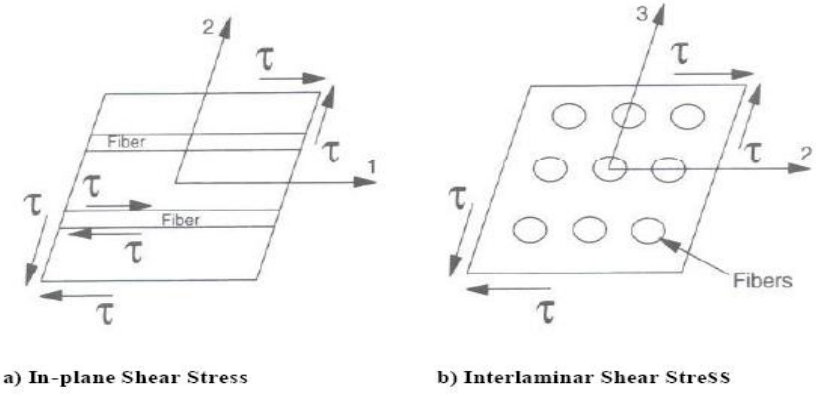

Figure (4): In-plane and Interlaminar Shear Stresses (Barbero E.J., 1999)

* ANSYS is highest quality engineering tools used to analyze the design with multiple applications

$$\begin{Bmatrix}\sigma_1\\ \sigma_2\\ \sigma_3\\ \tau_{23}\\ \tau_{13}\\ \tau_{12}\end{Bmatrix}=\begin{bmatrix}c_{11}\,c_{12}\,c_{13}\,c_{14}\,c_{15}\,c_{16}\\ c_{21}\,c_{22}\,c_{23}\,c_{24}\,c_{25}\,c_{26}\\ c_{31}\,c_{32}\,c_{33}\,c_{34}\,c_{35}\,c_{36}\\ c_{41}\,c_{42}\,c_{43}\,c_{44}\,c_{45}\,c_{46}\\ c_{51}\,c_{52}\,c_{53}\,c_{54}\,c_{55}\,c_{56}\\ c_{61}\,c_{62}\,c_{63}\,c_{64}\,c_{65}\,c_{66}\end{bmatrix}\begin{Bmatrix}\varepsilon_1\\ \varepsilon_2\\ \varepsilon_3\\ \gamma_{23}\\ \gamma_{13}\\ \gamma_{12}\end{Bmatrix} \qquad \textbf{….(2)}$$

The stress–strain relations in coordinates aligned with principal material directions are given by, (Yunus, S.M, Khonke, P.C.,1989):

$$\begin{Bmatrix}\sigma_1\\ \sigma_2\\ \sigma_3\\ \tau_{12}\\ \tau_{23}\\ \tau_{13}\end{Bmatrix}=\begin{bmatrix}c_{11}\;c_{12}\;0\;0\;0\;0\\ c_{21}\;c_{22}\;0\;0\;0\;0\\ 0\;0\;c_{33}\;0\;0\;0\\ 0\;0\;0\;c_{44}\;0\;0\\ 0\;0\;0\;0\;c_{55}\;0\\ 0\;0\;0\;0\;0\;c_{66}\end{bmatrix}\begin{Bmatrix}\varepsilon_1\\ \varepsilon_2\\ \varepsilon_3\\ \gamma_{12}\\ \gamma_{23}\\ \gamma_{13}\end{Bmatrix} \qquad \textbf{… (3)}$$

or

$$\{\sigma\}=[\mathrm{E}]\{\varepsilon\} \qquad \textbf{… (4)}$$

where

$c_{11} = \boldsymbol{A}\, E_{1,j}$ $\qquad$ $c_{33} = E_{3,j}\,B$

$c_{12} = \boldsymbol{A}\nu_{12}\, E_{1,j}$ $\qquad$ $c_{66} = G_{12,j}$

$c_{22} = \boldsymbol{A}\, E_{2,j}$ $\qquad$ $c_{44} = f\, G_{23}$ $\qquad$ $c_{55} = f\, G_{13}$

$\boldsymbol{A} = E_{2,j} / (E_{2,j} - \nu_{12,j} E_{1,j})$, $B = 10^{-6}$

$1/f$□$=1.2$

To obtain the stress–strain relations for the lamina of arbitrary orientation, the transformation equations are used for expressing stresses in ***x-y-z*** coordinate system in terms of stresses in ***1-2-3*** coordinate system (Calcote L.R., 1969):

$$\begin{Bmatrix}\sigma_x\\ \sigma_y\\ \sigma_z\\ \tau_{yz}\\ \tau_{xz}\\ \tau_{xy}\end{Bmatrix}=[\mathrm{T_m}]^{-1}\;[\mathrm{E}][\mathrm{T_m}]\begin{Bmatrix}\varepsilon_x\\ \varepsilon_y\\ \varepsilon_z\\ \gamma_{yz}\\ \gamma_{xz}\\ \gamma_{xy}\end{Bmatrix} \qquad \textbf{… (5)}$$

where

$$T_m = \begin{bmatrix} c^2 & s^2 & 0 & sc & 0 & 0 \\ s^2 & c^2 & 0 & -sc & 0 & 0 \\ 0 & 0 & 1 & 0 & 0 & 0 \\ -2sc & 2sc & 0 & c^2 - s^2 & 0 & 0 \\ 0 & 0 & 0 & 0 & c & -s \\ 0 & 0 & 0 & 0 & s & c \end{bmatrix} \quad \text{… (6)}$$

In which, $\boldsymbol{c} = \cos\theta$, $\boldsymbol{s} = \sin\theta$ and θ is the fiber orientation angle in degrees.

Using the above transformations, the stress–strain relations for arbitrary lamina orientation can be written as:

$$\begin{Bmatrix} \sigma_x \\ \sigma_y \\ \sigma_z \\ \tau_{yz} \\ \tau_{xz} \\ \tau_{xy} \end{Bmatrix} = \begin{bmatrix} Q_{11} & Q_{12} & 0 & Q_{14} & 0 & 0 \\ Q_{21} & Q_{22} & 0 & Q_{24} & 0 & 0 \\ 0 & 0 & Q_{33} & 0 & 0 & 0 \\ 0 & 0 & 0 & 0 & Q_{55} & Q_{56} \\ 0 & 0 & 0 & 0 & Q_{65} & Q_{66} \\ Q_{41} & Q_{42} & 0 & Q_{44} & 0 & 0 \end{bmatrix} \begin{Bmatrix} \varepsilon_x \\ \varepsilon_y \\ \varepsilon_z \\ \gamma_{yz} \\ \gamma_{xz} \\ \gamma_{xy} \end{Bmatrix} \quad \text{… (7)}$$

where:

$Q_{1j} = c^2 F_{1j} + s^2 F_{2j} - \mathbf{2}sc\, F_{4j}$ (j =1, 2, 4)

$Q_{21} = c^2 F_{2j} + s^2 F_{1j} + \mathbf{2}sc\, F_{4j}$ (j =1, 2, 4)

$Q_{33} = F_{33}$

$Q_{4j} = sc\, F_{1j} - sc\, F_{2j} + (c^2 - s^2) F_{4j}$ (j =1, 2, 4)

$Q_{5j} = c\, F_{5j} + s\, F_{6j}$ (j =5, 6)

$Q_{6j} = -s\, F_{5j} + c\, F_{6j}$ (j =2, 6)

$F_{11} = C_{11} c^2 + C_{12} s^2$ $F_{12} = C_{11} s^2 + C_{12} c^2$

$F_{14} = sc\,(C_{11} - C_{12})$ $F_{21} = C_{12} c^2 + C_{22} s^2$

$F_{22} = C_{12} s^2 + C_{22} c^2$ $F_{24} = sc\,(C_{12} - C_{22})$

$F_{33} = C_{33}$ $F_{41} = -\mathbf{2}sc\, C_{44}$

$F_{42} = \mathbf{2}sc\, C_{44}$ $F_{44} = C_{44}(c^2 - s^2)$

$F_{55} = cf\, C_{55}$ $F_{56} = -sf\, C_{55}$

$F_{65} = sf\, C_{66}$ $F_{66} = cf\, C_{66}$

A generally orthotropic composite lamina is an orthotropic lamina in which the principal material axes are not aligned with the structural axes and the constitutive matrix (**Q)** is as defined above in Equation (7).

2.4 Strain Displacement Relationship

The strain-displacement relationship can be written with its dependence explicitly expressed as:

$$\{\varepsilon\} = [B]\{u_i\} \quad \text{… (8)}$$

All elements of the strain–displacement matrix, $[B]$, are derived in terms of the shape function derivatives and the Jacobian matrix.

2.5 Element Stiffness Matrix

In general, the basic concept of the finite elements method is to discrete the continuum into a definite numbers of small elements connected together at their common nodes. The strain-displacement matrix, $[B]$, as shown previously is given by:

$\{\varepsilon\} = [B]\{u_i\}$, and therefore; the element stiffness matrix can be written as:

$$[k]^e = \int_V [\mathrm{B}]^T [\mathrm{E}][\mathrm{B}]\, dV = \int_{-1}^{1}\int_{-1}^{1}\int_{-1}^{1} [\mathrm{B}]^T [\mathrm{E}][\mathrm{B}] \det [J]\ dr\ ds\ dt \quad \textbf{… (9)}$$

in which,

$[\mathrm{K}]^e$: is the element stiffness matrix,

$|J|$: is the determinant of the Jacobian matrix.

For layered element, equation **(**9**)** can be written as (Yunus, et al 1989):

$$[K]^e = \int_{-1}^{1}\int_{-1}^{1}\sum_{j=1}^{N_1}\int_{r_j^{bt}}^{r_j^{tp}} [\mathrm{B}]^T [\mathrm{E}]_j [\mathrm{B}]\ dr \det [J]\ ds\ dt \quad \textbf{… (10)}$$

where**,**

N_1= number of layers.

r_j^{tp} and r_j^{bt} =coordinates of the top and bottom of the layer j, respectively.

2.6 Buckling Analysis

Linear buckling analysis in ANSYS finite-elements software is performed in two steps. The first step a static solution to the structure is obtained. In this analysis the prebuckling stress of the structure is calculated. The second step involves solving the eigenvalue problem given in form of Equation (11). This equation takes into consideration the prebuckling stress effect matrix [S] calculated in the first step (ANSYS®, 2004).

$$([K] + \lambda_i [S])\{\psi\}_i = \{0\} \quad \textbf{….(11)}$$

where $[k]$ = stiffness matrix

$[S]$ = Stress stiffness matrix

λ_i = ith eigenvalue (used to multiply the loads which generated [S])

$\{\psi\}_i$ = ith eigenvector of displacements.

The ‘Block Lanczos’ method was used to extract the eigenvalue resulting from Equation (11). The buckling analysis was done to obtain the cylinder failure behavior under which give an idea on the ability of use of the composite cylinder in different application in different load manner. In addition to define the region of failure to deal

it carefully. The critical buckling load of the model presents the more important index in the buckling analysis.

3. The flow-chart of the Computer Program.

The flow-chart of the computer program **ANSYS V9.0** that is used in this research will be summarized in Figure (5) below.

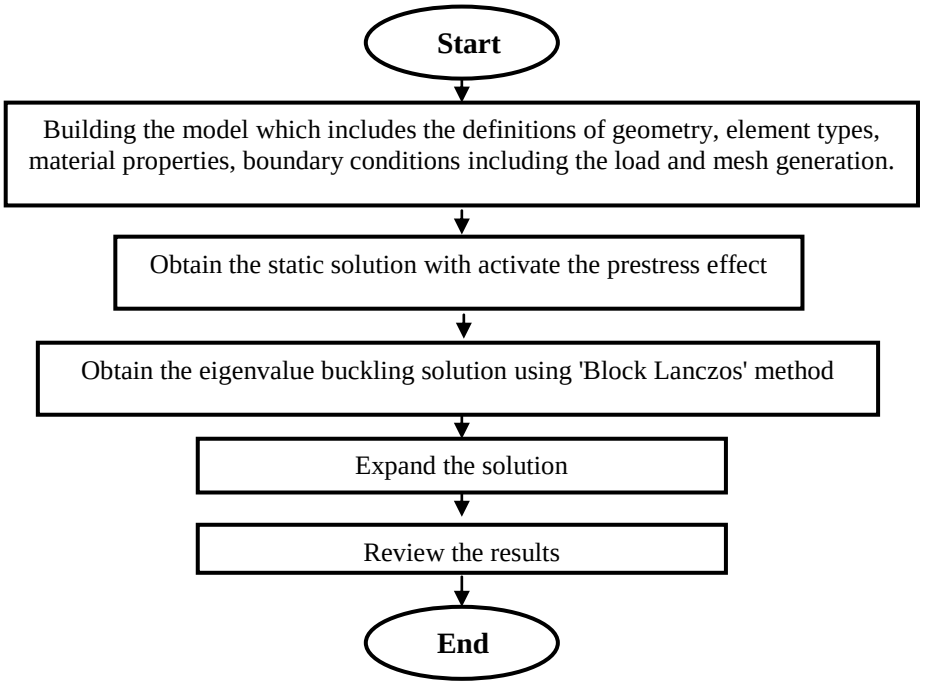

Figure (5): The flow-chart of the computer program.

4. Results and Discussion

Effect of several parameters are investigated for a six layers, eight stringer stiffeners and six ring stiffeners with cross section (6*3 mm^2) stiffened composite cylinder of 180 mm in length and 146 mm in diameter for a style of stacking sequence (90/-θ/+θ).

Table 1: Macromechanical Properties of Stiffened Layers in a Laminate glass/ epoxy (Jones, R.M, 1999)

E_1 **GPa**	$E_2=E_3$ **GPa**	v_{12}	G_{12} **GPa**	$G_{23}=G_{13}$ **GPa**	$v_{13}= v_{23}$	***Density,*** ρ kg/m^3
54	18	0.25	9	11.5	0.083	1940

4.1 Effect of Shell Thickness

The effect of shell thickness on buckling load was investigated using the finite elements model.Ten analyses were performed to smoothly increase the skin thickness from 0.5 mm to 7 mm. Figure (6) shows plot of the results obtained from these analyses for winding angle sequence of 90/-15/+15.

It is observed that the buckling resistance of the stiffened cylinder steadily increases with increase in shell thickness. Even though a steady increase in buckling load is observed with skin thickness increase, the gain per mass added reaches a

maximum and then declines after a certain point (Figure (7)) because the increase in mass is larger than the increase in the strength of the cylinder as depicted. The gain per mass measures the efficiency of the mass added, i.e., the additional load carried by the added mass.

For the analysis performed on the stiffened cylinder, the optimum skin thickness at which the specific load (load per mass) reaches maximum is found to be 2.48 mm (Figure 7). It can be observed from the same figure that the optimum skin thickness lies in the global buckling failure mode region. This result is very significant as it confirms the observation of other researchers, (Brian, F. T. (1998), and Mostafa, N. H., Waheed, S. O. (2008)) that only global buckling failure mode results in the maximum specific buckling load, and consequently leads to the conclusion that the global buckling failure mode should be the design criteria for a stiffened cylinder and it must be taken in the considerations.

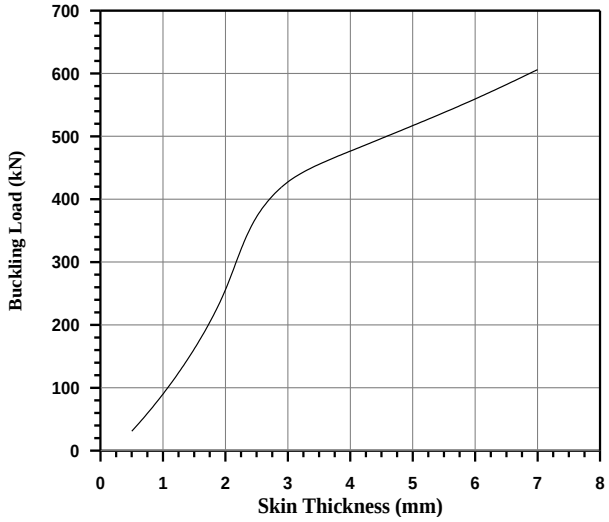

Figure (6): Buckling load due to increase the skin thickness

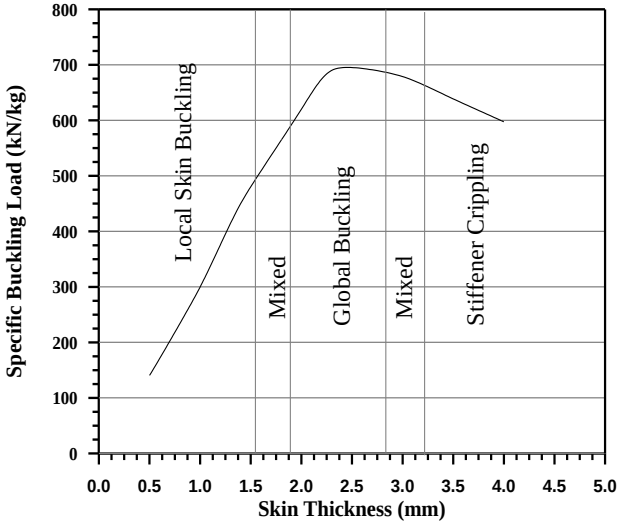

Figure (7): Specific buckling load under different buckled regions

The cylinder with the thinnest shell thickness of 0.5 mm up to 1.53 mm was observed to fail purely due to local skin buckling Figure **(**8a) where the stiffness is largely depends on the thickness value. When the skin thickness was increased, the failure mode gradually changed to global buckling at about 1.85 mm skin thickness. At this point in addition to local buckling of the skin, the adjacent stiffeners started to buckle as well. With further skin thickening of the shell, the localized skin and stiffener failure spread to adjacent cells and gradually transformed to a more global buckled failure mode Figure **(**8b). At about a skin thickness of 3.23 mm, the shell was observed to be relatively stronger than the stiffeners and hence localized stiffener crippling started to occur. For any skin thickness more than 3.23 mm the local stiffener crippling failure mode prevailed Figure **(**8c).

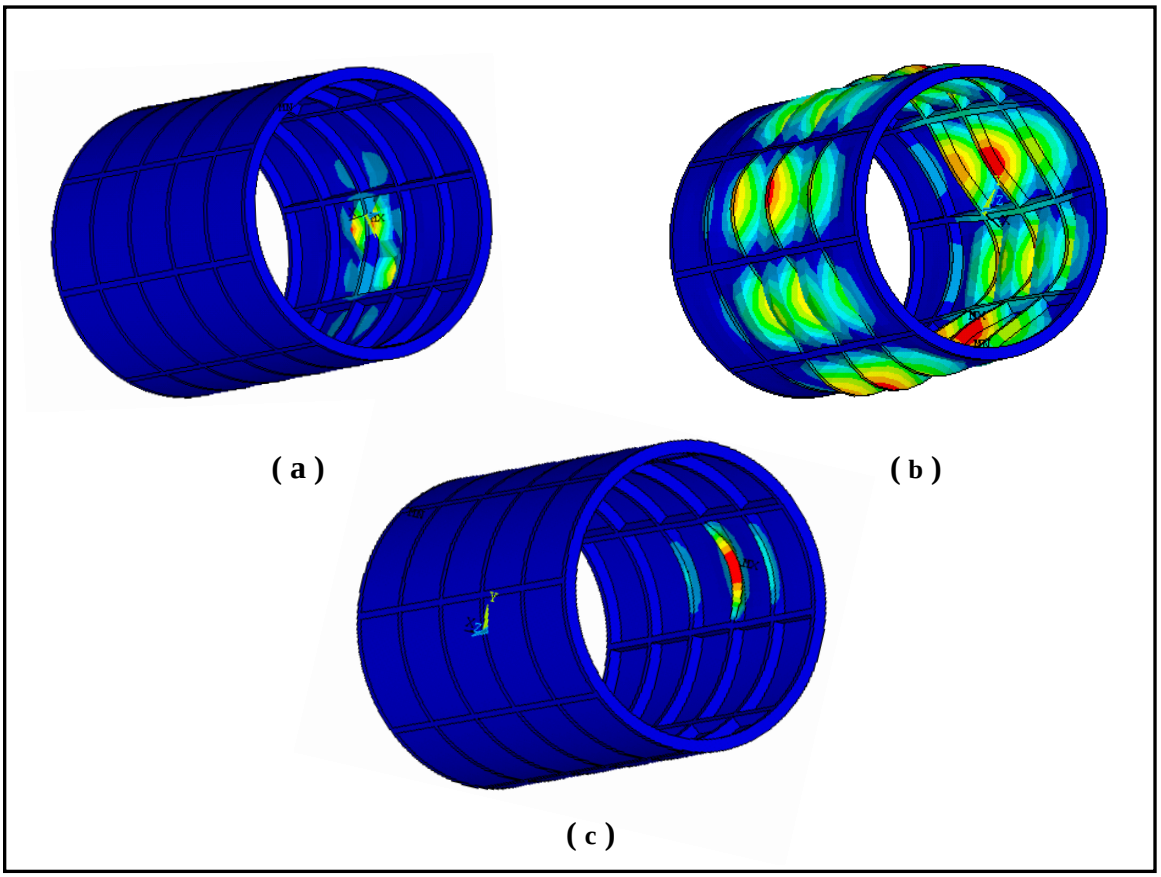

Figure(8): Buckling failure modes :(a) local skin buckling, (b) global buckling ,(c) local stiffener crippling.

Figures (9) and (10) that found by Mostafa, N. H. and Waheed, S. O. (2008) used a composite cylinder with only stringer stiffeners. Kidane, S., (2002) used finite elements method to find the critical buckling load and the specific load with thickness for a composite cylinder with grid stiffeners as shown in Figure (11). It should be noted that the problem dimensions and material properties that used by, N. H. and Waheed, S. O. (2008) and Kidane, S., (2002) were different from the present research, but the behavior of the results are the same when they compared with present study.

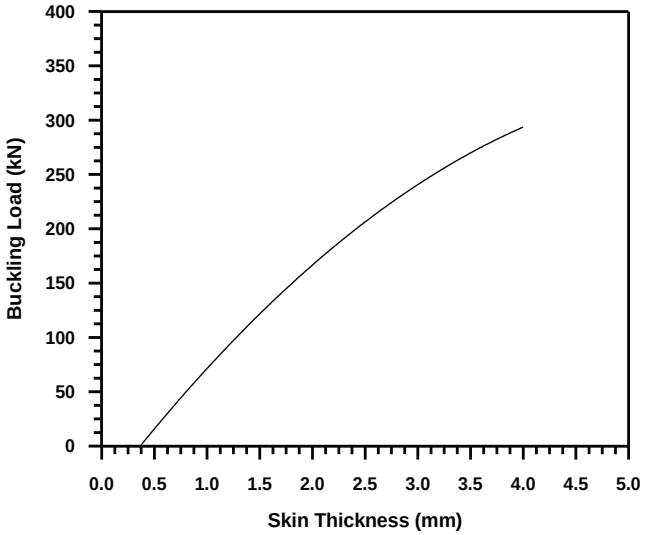

Figure (9): Buckling load due to increase the skin thickness Mostafa, N. H. and Waheed, S. O. (2008)

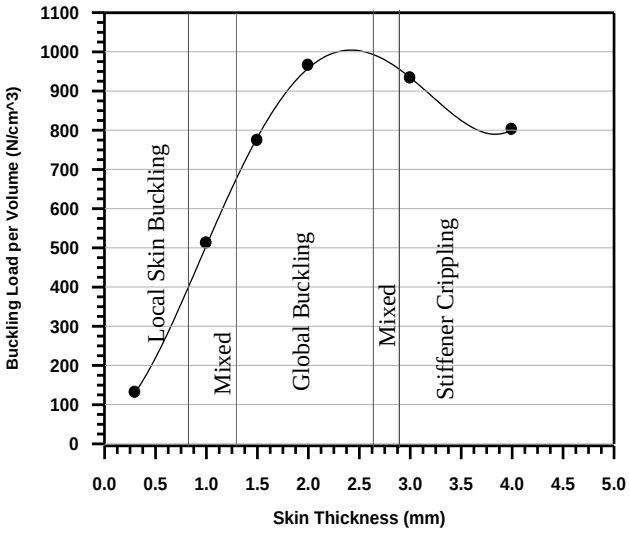

Fig.(10): Buckling load under different buckled regions Mostafa, N. H. and Waheed, S. O. (2008)

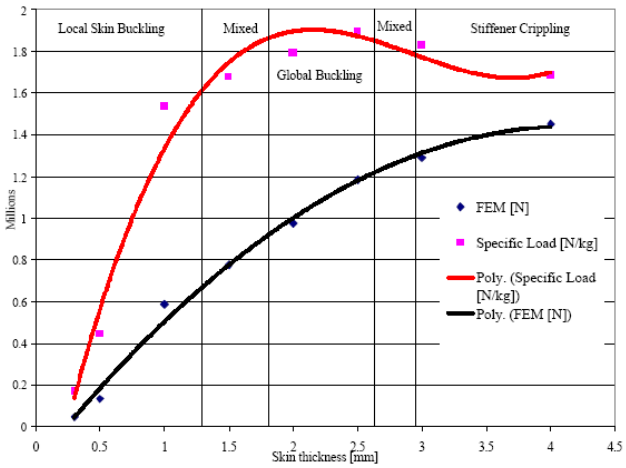

Figure (11): Buckling load and specific buckling load with thickness, Kidane, S., (2002).

4.2 Effect of Shell Winding Angle

Shell winding angle is one of more important design variables that can be easily varied using the finite-elements model. The shell winding angle can be varied by just changing the inputs of the real constants table, without changing the model. The effect of shell winding angle was investigated for the three types of buckling failure modes. The analysis was performed on models having skin thickness of 0.5 mm, 2.4 mm and 4.5 mm. These three skin thicknesses correspond to local skin buckling, global buckling and stiffener crippling failure modes respectively. The analyses results are presented in Figure (12) below.

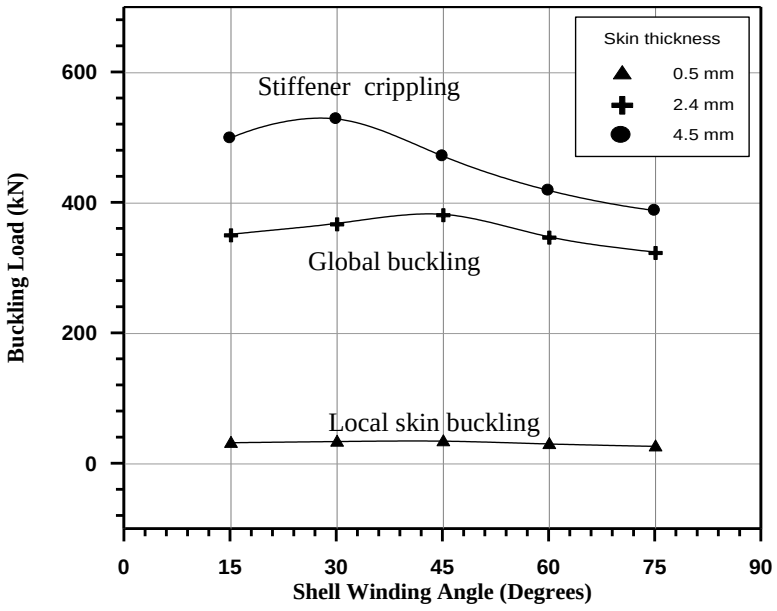

Figure (12): Effect of shell winding angle on buckling load

It can be observed that the variation in shell winding angle has different effects on each type of failure modes. For local skin buckling failure mode, which corresponds to 0.5 mm skin thickness curve, it is clear that buckling load seems insensitive to changes in shell winding angle and show almost flat curves for buckling load versus

mat orientation. While, the optimum shell winding angle for a stiffened cylinder failing in stiffener crippling failure mode is about 30^o. The buckling load resistance increases steadily with winding angle increment. On the other hand, for global buckling failure mode (2.4 mm skin thickness), with increase in shell winding angle the load resistance of the structure first increases and then goes down after reaching a maximum. Hence, it was concluded that there exists an optimum shell winding angle for a stiffened cylinder failing in global buckling failure mode. The optimum shell winding angle for a stiffened cylinder having a skin thickness of 2.4 mm is found to be about 45^o.

4.3 Effect of Modulus

The effect of modulus on the buckling load of a stiffened composite cylinder was investigated using ANSYS package. The analysis was performed for a wide range of skin thickness. It has been shown in ***Section 4.1*** that buckling failure mode highly depends on the skin thickness.

The longitudinal modulus of the composite system was varied from **54 GPa** to **100 GPa** depending on the temperature and volume fraction (Valery, V., Evgeny, V., 2001). The effect of modulus was studied on stiffened cylinders having shell thickness varying from 0.5 mm to 3.5 mm with shell winding angle equal to 15°. Figure (13) below summarizes the results obtained. The buckling load was observed to increases linearly with increase in longitudinal modulus for all skin thickness. It appears from the plot that the gain in buckling resistance increases as the skin thickness increases. But a close look at **Table (2)**, which tabulates the percentage gain in the buckling load with increase in modulus, shows a higher gain in buckling load is obtained for a skin thickness 2 mm (global buckling mode) .Hence it can be concluded that a better gain in buckling load resistance is achieved if the longitudinal modulus is increased for a stiffened cylinder failing in global buckling failure mode than for a stiffened cylinder failing in a stiffener crippling failure mode or in local skin buckling failure mode.

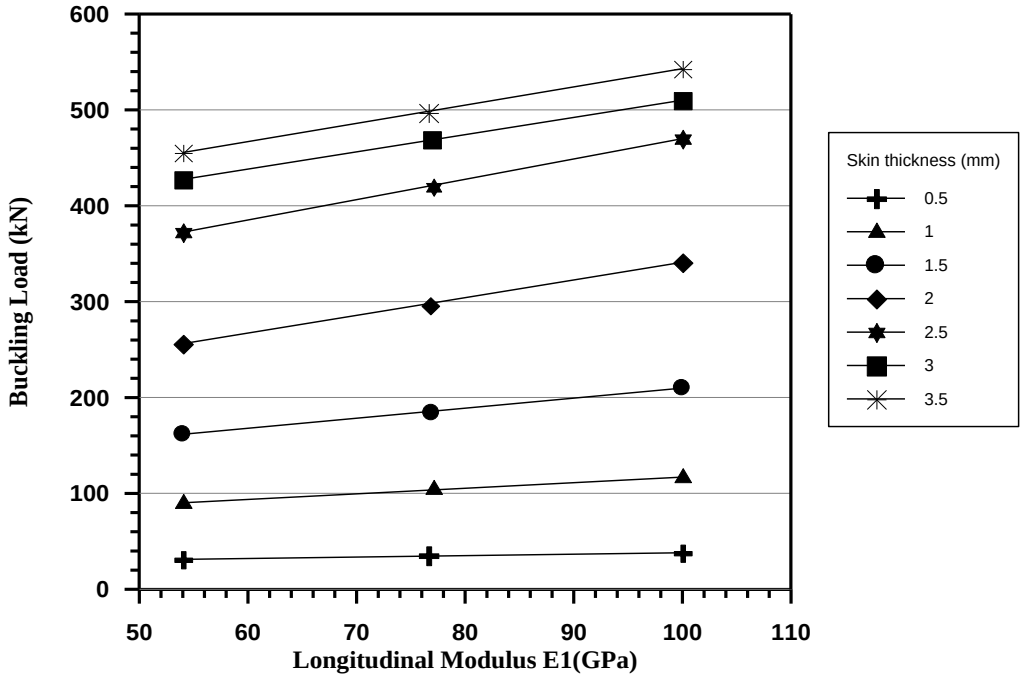

Figure (13): Effect of longitudinal modulus on buckling loads.

$$where \quad \%Load \quad gain = \left(\frac{Buckling \quad Load_{E1=100} - Buckling \quad Load_{E1=54}}{Buckling \quad Load_{E1=54}} \right) * 100 \qquad \textbf{…(12)}$$

Table (2): Gain in buckling load with thickness increases

Skin thickness	0.5 mm	1 mm	1.5 mm	2 mm	2.5 mm	3mm	3.5 mm
% Load gain	21.97	29.74	29.76	33.12	26.21	19.32	19.2

Conclusions

In the buckling analysis of stiffened composite cylinders, a number of important problems remain to be resolved. In this paper, attention has been paid to include several parameter that affect the buckling behavior of the problem within hand such as fiber orientation, shell thickness, and elastic material properties. Three different failure modes named global buckling, local skin buckling, and stiffener crippling were studied with different parameters. Each failure mode gave different results of the other mode, and the results were compared to find optimum design of the stiffened composite cylinder. The numerical results presented herein show that global buckling failure mode was the optimum design criteria of the stiffened composite cylinder.

References

Barbero, E.J., 1999," Introduction to Composite Material Design", Taylor & Francis, Philadelphia, PA.

Brian, F. T., 1998, "Analysis and Design of Variable Stiffness Composite Cylinders" Ph.D. Thesis, Virginia Polytechnic Institute and State University, Blacksburg, Virginia, USA.

Calcote, L. R., 1969, "The Analysis of Laminated Composite Structures", Van-Nostrand Reinhold, New York.

Graham, j., 1993," Preliminary Analysis Techniques for Ring and Stringer Stiffened Cylindrical Shells", NASA report TM-108399.

Horak,J., Lord, G. J.,and Peletier,M.A., 2005," Cylinder Buckling: the Mountain Pass as an Organizing Center" arXiv:math.AP/0507263 V1.

Hatem , H. O., 2002, "Investigation of Performance and Optimum Design of Fiber-Reinforced Composite Shell of Aircraft Structure", ", Ph.D. Thesis, The Military College of Engineering , Baghdad, Iraq.

Stegman, J., and Lund , L, 2002, "Notes on Structural Analysis of Composite Shell Structure", First Edition.

Jones, R. M., 1999, "Mechanics of Composite Materials", Second Edition, Taylor & Francis, Inc..

John, L., Melvin, S., and Robert, L., July 1972, "Optimum Mass-Strength Analysis for Orthotropic Ring-Stiffened Cylinders Under Axial Compression" NASA TN D-6772.

Kidane, S., 2002 " Buckling Analysis of Grid Stiffened Composite Structures" M.Sc. Thesis, Louisiana State University,USA.

Knight N.F., Stranes J.H. , 1997, "Development in Cylindrical Shell Stability Analysis," NASA report.

Langley, P. T., 1998, "Finite Element Modeling of Tow-Placed Variable-Stiffness Composite Laminate", M.Sc. Thesis, Virginia Polytechnic Institute and State University, Virginia, U.S.A.

Mostafa, N. H and Waheed, S. O., 2008,"Buckling Analysis of Stringer Stiffened Composite Cylinder" The Iraqi Journal for Mechanical & Materials Engineering .

Phillips, J.L., Gurdal, Z., 1990, “Structural Analysis and Optimum Design of Geodesically Stiffened Composite Panels,” NASA Report CCMS-90-05 July .

Valery, V., Evgeny, V., 2001 “Mechanics and Analysis of Composite Materials” First edition, Elsevier Science Ltd**.**

Venkataraman, S. , 1999, " Modeling, Analysis and Optimization of Cylindrical Stiffened Panels for Reusable Launch Vehicle Structures" Ph.D. Thesis, University of Florida, USA.

Yunus, S. M., and Khonke, P. C. , 1989, “An Efficient Through-Thickness Integration Scheme in an Unlimited Layer Doubly Curved Isoparametric Composite Shell Element”, International Journal for Numerical Methods in Engineering, Vol. 28, p.p. 2777-2793.

ANSYS®, Engineering Analysis System Theoretical Manual, “Http:\\ www. Ansys. Com”, Ansys Version 9.0, 2004.